GROWTH OF FLUORINE DOPED ZINC OXIDE NANOSTRUCTURES FOR ULTRA-VIOLET PHOTODETECTOR USING MODIFIED CHEMICAL BATH-HYDROTHERMAL METHOD

MUHAMMAD AMINU

UNIVERSITI SAINS MALAYSIA

2022

GROWTH OF FLUORINE DOPED ZINC OXIDE NANOSTRUCTURES FOR ULTRA-VIOLET PHOTODETECTOR USING MODIFIED CHEMICAL BATH-HYDROTHERMAL METHOD

by

MUHAMMAD AMINU

Thesis submitted in fulfilment of the requirements
for the degree of
Doctor of Philosophy

September 2022

ACKNOWLEDGEMENT

All praises and gratitude are due to Allah, most merciful and most beneficent. Many thanks to my main supervisor, Professor Dr. Zainuriah binti Hassan, for her time, advice, guidance, criticisms and assistance during this research journey. I have had the good fortune of working under someone whose enthusiasm for research is contagious.

I am also very grateful to my co-supervisor, Dr. Sabah M. Mohammad, for his guidance, time, comments, and brotherly suggestions and I would like to thank him for being with me throughout this PhD journey.

This thesis is dedicated to my beloved family, my father Muhammad Wada bn Hashim, my mother Hauwa Alhassan, my brothers and sisters, my stepmothers, maternal and paternal uncles and aunties, my wife and children. Moreover, I really appreciate my wife (Amina Isyaku Wakili) and my kids (Maryam, Abdullahi, and Asiya) for their sacrifices in my long absence from them to acquire this degree. This PhD journey would not be possible without your immense prayers, encouragement, concerns, and support.

I acknowledge Sule Lamido University, Kafin-Hausa, Jigawa State, Nigeria for this research scholarship under the Nigerian government tertiary fund (Tet-Fund) agency and the support from Universiti Sains Malaysia is also acknowledged. Finally, I would like to express my gratitude to the INOR staff, NOR lab. staff (teaching and non-teaching), and staff of Physics Department at Sule Lamido University for their prayers, co-operation, suggestions, technical assistance and valuable contribution to my work.

Muhammad Aminu
Penang, Malaysia, 2022.

TABLE OF CONTENTS

LIST OF TABLES

Page

LIST OF FIGURES

Page

LIST OF SYMBOLS

α	Absorption coefficient
$\boldsymbol{a}$, $\boldsymbol{b}$ & c	Lattice constants
$\boldsymbol{b'_1, b'_2, b'_3}$	Three types of second-nearest-neighbour distances
Ag	Silver
F	Fluorine
OD	Optical density
K	Extinction coefficient
O	Oxygen
O_i	Oxygen interstitial
O_v/V_o	Oxygen vacancy
O_{Zn}	Oxygen antisite
Si	Silicon
Zn	Zinc
Zn_i	Zinc interstitial
Zn_v	Zinc vacancy
e/q	electronic charge
I_{dark},	Dark current
I_{ph}	Photocurrent
P_{in}	Incident illuminated power
A	Irradiated area
η	External quantum efficiency
c	Velocity of the light and wavelength of incident light
$\boldsymbol{D^*}$	Detectivity
τ_r/τ_f	Rise/Fall times
D	Crystallite size

λ	X-ray wavelength
θ	Bragg diffraction angle
β	Full width at half maximum
d	Interplanar spacing between the planes in the atomic lattice
I_{UV}/I_{DLE}	Ratio of the intensity of UV emission to the visible deep level emission
$F(R)$	Kubelka Munk function.

LIST OF ABBREVIATIONS

AFM	Atomic Force Microscope
ALD	Atomic layer deposition
CBD	Chemical bath deposition
CB	Conduction band
DI	De-ionized
DLB	Duran laboratory bottle
DLE	Deep-level emission
EDX	Energy Dispersive X-ray
F	Fluorine
FESEM	Field emission scanning electron microscopy
FAZO	F and Ag co-doped ZnO
FWHM	Full width at half maximum
FZO	F-doped ZnO
GID-XRD	Grazing Incidence Diffraction X-ray Diffractometer
HMT	Hexamethylenetetramine
MCB-HM	Modified chemical bath-hydrothermal method
MSM	Metal Semiconductor Metal
NBE	Near band emission
NFLs	Nanoflowers
NMSs	Nano-to-microstructures
NR	Nanorod
NS	Nanostructure
NWs	Nanowires
PAT	Post annealing temperatures
PET	Polyethelene naphthalate

PD	Photodetector
PL	Photoluminescence
SEM	Scanning electron microscopy
TCO	Transparent conductive oxide
TEM	Transmission electron microscopy
THG	Third harmonic generation
TSC	Trisodium citrate
UV	Ultraviolet
VB	Valence band
XPS	X-ray photoelectron spectroscopy
XRD	X-ray diffraction
ZnO	Zinc oxide

PERTUMBUHAN NANOSTRUKTUR ZnO YANG DIDOP FLUORIN UNTUK PENGESAN FOTO ULTRA-UNGU MENGGUNAKAN KAEDAH HIDROTERMA-RENDAMAN KIMIA YANG DIUBAHSUAI

ABSTRAK

Matlamat utama penyelidikan ini adalah penggunaan kaedah hidroterma-rendaman kimia yang diubahsuai untuk sintesis ZnO yang tidak didop dan didopkan dengan fluorin (FZnO) untuk aplikasi pengesan foto (PD) ultra-ungu (UV). Kesan kepekatan fluorin (F) dalam sifat ZnO telah disiasat pada substrat Si, yang mengakibatkan peningkatan kualiti kristal, sifat optik dan elektrik ZnO pada kepekatan F rendah. Seterusnya, pengesan foto UV logam-semikonduktor-logam (MSM) telah difabrikasikan berdasarkan ZnO yang tidak didop dan FZnO yang dioptimumkan. Jika dibandingkan dengan peranti ZnO yang tidak didop, sifat peranti pengesan foto FZnO yang dioptimumkan telah dipertingkatkan dengan ketara dengan cahaya UV 395 nm. Nilai arus foto, respontiviti, kepekaan, pengesanan, masa naik dan masa jatuh peranti ZnO yang tidak didop adalah masing-masing 3.61 μA, 0.22 A/W, 9.7 x10^{3}%, 2.2 x10^{19} Jones, 1.9 s dan 1.7 s. Parameter untuk peranti FZnO, sebaliknya, telah bertambah kepada 10.52 μA, 0.66 A/W, 1.1x10^{5}%, 1.3x10^{10} Jones, 90 ms dan 110 ms, masing-masing. Oleh itu, nanorod (NRs) FZnO yang disintesis menggunakan kaedah hidroterma yang diubah suai mendedahkan penemuan cemerlang yang bermanfaat dalam reka bentuk dan pembuatan peranti UV MSM PD yang murah untuk pelbagai aplikasi optoelektronik. Di samping itu, kesan trisodium sitrat (TSC) pada FZnO telah disiasat. Mikroskopi pengimbasan elektron pancaran medan (FESEM) mendedahkan struktur nanorod (NRs) yang dijajarkan secara menegak, seperti batu kerikil dan seperti struktur blok dengan saiz yang berbeza

dengan penambahan TSC. Pertumbuhan sepanjang paksi-c telah dihalang dan sepanjang paksi-a telah dibangunkan dengan penambahan TSC seperti yang didedahkan oleh pembelauan sinar-X (XRD). Kedua-dua keputusan analisis UV-cahaya nampak dan fotoluminesen (PL) adalah selaras antara satu sama lain, menunjukkan anjakan biru jurang jalur tenaga dan peningkatan kualiti kristal telah disahkan menggunakan analisis PL dengan penambahan TSC. Selanjutnya, kesan pengedopan bersama perak dan fluorin pada sifat ZnO telah disiasat. FESEM mendedahkan NRs yang dijajarkan secara menegak dengan panjang dan diameter berbeza selepas pengedopan bersama. Kenaikan saiz kristal dan pengurangan mikroterikan telah didedahkan oleh XRD dengan pengedopan bersama. Juga, kecacatan yang boleh dilihat telah dikurangkan dengan ketara dengan pengedopan bersama, mengesahkan peningkatan kualiti kristal seperti yang didedahkan daripada analisis PL dan XRD. Akhirnya, penambahan pinggir penyerapan dalam UV-C telah direalisasikan dengan pengedopan bersama, memberikan isyarat yang kuat untuk digunakan dalam pengesanan UV-C yang sangat sukar dengan hanya bahan ZnO. Analisis spectroskopi fotoelektron x-ray (XPS) mengesahkan kehadiran perak, fluorin, zink dan oksigen dalam sampel. Akhirnya, dua PD berdasarkan ZnO yang didop fluorin (FZO) dan pengedopan bersama fluorin, perak (FAZO) telah difabrikasikan. PD FAZO mengatasi prestasi PD FZO dari segi ciri tindak balas foto pada voltan pincang yang lebih rendah apabila disinari dengan cahaya UV 365 nm yang mungkin berkaitan dengan kualiti kristal yang lebih baik dalam PD FAZO. Kepekaan, respontiviti, kecekapan kuantum, pengesanan, masa naik dan turun pada pincang sifar untuk PD FAZO ialah 24463%, 8.24 mA/W, 6.47×10^{8} Jones, 2.8%, 70 ms dan 80 ms, masing-masing, dan 9418%, 0.2 mA/W, 6.25×10^{7} Jones, 0.1%, 80 ms dan 80 ms untuk PD FZO. Oleh itu, pengedopan dengan F, pengedopan bersama F

dan Ag dalam ZnO menunjukkan keputusan yang menjanjikan peningkatan ciri parameter PD yang boleh digunakan dalam opto-elektronik.

GROWTH OF FLUORINE DOPED ZINC OXIDE NANOSTRUCTURES FOR ULTRA-VIOLET PHOTODETECTOR USING MODIFIED CHEMICAL BATH-HYDROTHERMAL METHOD

ABSTRACT

The main aim of this research work was the use of modified chemical bath-hydrothermal method for the synthesis of undoped and fluorine doped zinc oxide (FZnO) for ultra-violet (UV) photodetector (PD) application. The effect of fluorine (F) concentration in ZnO properties was investigated on Si substrate, which resulted in enhancement of the crystal quality, optical and electrical properties of ZnO at low F concentration. Subsequently, UV metal-semiconductor-metal (MSM) PD was fabricated based on the undoped ZnO and optimized FZnO. When compared to an undoped ZnO device, the photodetection properties of the optimized FZnO device were enhanced appreciably using the UV-light of 395 nm. The value of photocurrent, responsivity, sensitivity, detectivity, rise time and fall time of the undoped ZnO device were 3.61 μA, 0.22 A/W, 9.7 $x10^3$%, 2.2 $x10^{19}$ Jones, 1.9 s and 1.7 s, respectively. The parameters for the FZnO device on the other hand, were increased to 10.52 μA, 0.66 A/W, $1.1x10^5$%, $1.3x10^{10}$ Jones, 90 ms and 110 ms, respectively. Hence, FZnO nanorod (NRs) synthesized using modified hydrothermal method revealed outstanding findings which could be extremely beneficial in the design and manufacture of inexpensive UV MSM PD devices for a variety of optoelectronic applications. In addition, the impact of the trisodium citrate (TSC) on FZnO was investigated. Field emission scanning electron microscopy (FESEM) revealed vertically aligned NRs, pebble-like and block-like structures of different sizes upon TSC addition. The c-axis growth was inhibited and that of a-axis was developed

upon TSC addition as revealed by X-ray diffraction (XRD). Both UV-Visible and photoluminescence (PL) analyses results conforms to each other, showing blue-shift of energy bandgap and enhancement of crystal quality was confirmed using PL analysis upon TSC addition. Furthermore, the effect of silver and fluorine co-doping on ZnO properties was investigated. The FESEM revealed vertically aligned NRs of different lengths and diameters after co-doping. The crystallite size increment and microstrain decrement were revealed by XRD upon co-doping. Also, visible defects were suppressed significantly with the co-doping, confirming enhancement of crystal quality as revealed from PL and XRD analyses. Finally, additional absorption edges in UV-C were realized upon co-doping, giving a great signal for employment in UV-C detection which is very difficult with the only ZnO material. X-ray photoelectron spectroscopy (XPS) analysis confirmed the presence of silver, fluorine, zinc and oxygen in the samples. Finally, two PDs based on fluorine doped ZnO (FZO) and fluorine, silver co-doped (FAZO) were fabricated. The FAZO PD outperformed the FZO PD in terms of photoresponse characteristics at even lower bias voltages, when irradiated with the UV-light of 365 nm, which might be related to better crystal quality in the FAZO PD. The sensitivity, responsivity, quantum efficiency, detectivity, rise and fall times at zero bias for the FAZO PD are 24463%, 8.24 mA/W, 6.47×10^{8} Jones, 2.8%, 70 ms, and 80 ms, respectively, and 9418%, 0.2 mA/W, 6.25×10^{7} Jones, 0.1%, 80 ms, and 80 ms for the FZO PD. Hence, F-doping, F and Ag co-doping in ZnO showed promising results for the enhancement of PD parameters characteristics employable in opto-electronics.

CHAPTER 1

INTRODUCTION

1.1 General Introduction

Intentional introduction of impurities into intrinsic material (semiconductor) is promising, excellent, very useful, reliable for the improvement of fundamental characteristics of the material; the process known as doping. Zinc Oxide (ZnO) is one of the most important, promising, interesting, widely applicable semiconductor with unrivaled properties like high transparency in the visible light range due to its huge wide direct energy bandgap of 3.37eV and huge exciton binding energy of approximately 60 meV at room temperature (RT), outstanding low resistance, with the composition of zinc and oxygen which are naturally abundant in large quantity [1], [2]. The ZnO powder color is white at RT and changes to yellow when heated, this color change was due to oxygen lost at high temperature [3]. It receives dopant impurities or vacancies to tune/tailor its physical, chemical, thermal properties for different optoelectronic device applications depending on the requirement for that particular device. Moreover, among many merits of ZnO is its biocompatible, low cost/cheap, thermally and chemically stable, environmentally non-harmful as well as its operation in the unpleasant environment and large temperature were among the reasons for the employment in many applications [1], [4]–[6]. The potential and promising nature of ZnO make it widely used over other metal oxides in various applications, including solar cells [7], [8], light emitting diode [9], gas sensor [1] photocatalytic activity [10], transparent conducting oxide [11], ultra-violet (UV) photodetector (PD) [12]–[14].

The great mechanical and thermal stability, high sensitivity, and simplicity in making variety of morphologies at the both micro-nanoscales make ZnO even more attractive. The metal oxide like ZnO can be used to fabricate a device that is resistant and responsive to high-temperature without electrical deterioration. In addition, there are more advantages of ZnO over gallium nitride (GaN), including the availability of relatively high-quality ZnO bulk single crystals and a significant exciton binding energy of 60 meV. ZnO also offers a significantly easier crystal-growth process, which means ZnO-based products could be cheaper [15].

However, doping is promising for the improvement and enhancement of the characteristics, properties of semiconductors for better device performance. The efficient and enhanced characteristic parameters of both doped ZnO PDs and solar cells have been reported in several previous studies [4], [16]–[18]. ZnO nanostructures (NSs) have been widely doped with both anions and cations employing different procedures, such as chlorine-doped ZnO prepared by the solution method [18], [19], zirconium-doped ZnO fabricated by atomic layer deposition (ALD) and sol-gel method [20], [21], phosphorus-doped ZnO grown by the hydrothermal method [22], vanadium-doped ZnO prepared by the hydrothermal method [23], manganese-doped ZnO fabricated by the hydrothermal process [24], nickel/copper co-doped ZnO synthesized by the hydrothermal method [5]. The hydrothermal method is cheap, simple, occurs at a relatively low temperature, and can be deposited on different types of substrate including flexible substrate [1], [9], [25]. Furthermore, it is well known, halogen doping reduces the oxygen surface adsorption/ desorption. Fluorine (F) being a member of the halogen group is one of the most electronegative elements, an anion dopant, consumer of oxygen defect, can readily be incorporated into ZnO matrix due to closely compatible ionic radius of F^-

(0.136 nm) with O^{2-} (0.140 nm) with the minimally reduced lattice distortion to improve electron transport properties in ZnO nanorods (NRs) [17], [26]. Fluoride ion (F^-) can promote solubility of the precursors efficiently, improve solution chemical potential which subsequently favours nanostructure (NS) growth, and minimize material resistance for better conductivity. Also, F^- enhances the carrier's mobility ions by decreasing the viscosity of the solution to attain improved conductivity and hinders recombination by not trapping electrons [27]–[33]. The rate of scattering is improved by F-doping due to grain boundary density increment [34].

UV light of a wavelength in the range of 10 to 400 nm is electromagnetic radiation. These waves have wavelengths that fall between visible light and X-rays. Because it comprises electromagnetic waves with frequencies higher than those associated with the violet colour, the spectrum is termed "ultraviolet". International Commission on Illumination classified the UV spectrum into three regions: UV-A (400–320 nm), UV-B (320–280 nm), and UV-C (10–280 nm) [13], [35], [36]. UV radiation with a wavelength of less than 280 nanometers is damaging to the biosphere because it may cause skin cancer, irritation in the eyes and premature aging in humans and immune system damage. As a result, a material that will absorb light in this entire range for photodetection applications is needed to reduce uncontrolled exposure to this radiation. Because UV-A radiation (320-400 nm) has a high penetration rate, it can reach the ground and is referred to as the UV window of the atmosphere. Hence, uncontrolled long exposure to UV increases due to industrialization and air pollution in developed countries, causing various health risks and damages. Therefore, it is crucial and necessary to use effective UV photodetectors to monitor the degree of UV light intensity that is unsafe on human skin while engaging in daily activities. An ideal UV detector must have a low-cost

and easy fabrication process, as well as high sensitivity, repeatability, good responsivity, fast response times and low noise for subsequent application in in the medical, UV imaging, emission sensors, and other sectors [4], [37], [38].

1.2 Problem Statement

Thin-film material provides additional grain boundaries that hinder charge carriers in the process of direct transport pathway resulting in low crystal quality in terms of structure which is unfavorable for the PD fabrication. The photocurrent does not rapidly attain a steady state in terms of the rise and fall processes due to more grain boundaries in the thin film. Nano-structured materials such as 1-dimensional (1D) ZnO nanostructures (NSs) which include nanorods (NRs), nanowires (NWs), and nanoneedles (NNs) offer better unmatched and tunable electrical, optical, chemical, mechanical properties as compared to the thin and bulk film [39], [40]. These properties are very important in the realization of efficient optoelectronic devices. In particular, 1D ZnO NRs have demonstrated a remarkable potential in photovoltaic applications as such they are preferred because of their huge surface state density for enhancement of life carrier time and low reflectivity, large surface-to-volume ratios, huge capable carrier charge collection, and quantum confinement effects which improve many photon interactions resulting in improvement of absorption ability by reflection suppression in photovoltaic applications [13], [25], [41], [42].

However, ZnO NRs demonstrate a large oxygen adsorption/desorption process resulting in dark current decrement and responsivity increment of the ZnO-based UV devices which subsequently lead to a very long response and decay time [12]. Also, ZnO NRs display weak ultraviolet signals because of huge dark current,

high electron-hole pair rate recombination and these will have a serious effect in realizing very efficient optoelectronic devices [13], [43], [44]. Therefore, 1D ZnO-based UV PD has a long rise and fall time due to the oxygen-related hole-trap states on the NRs surface [45]. To minimize and solve these problems, 1D ZnO doping is employable to tune, improve the electrical, optical, chemical, mechanical properties which can significantly provide a proper solution in the enhancement of ZnO-based optoelectronic devices. Anionic or cationic doping may be used, but, the latter perturbs the conduction band (CB) minimally, while the former plays a critical role in minimizing electron scattering in the CB, thus maximizing electron transport and, as a result, increasing conductivity [11]. In the midst of the anionic dopant, fluorine being the most electronegative element (3.98) is the most promising anion dopant which consumes oxygen defects, and can easily be integrated into the ZnO matrix to substitute O with the minimal perturbation due to relatively nearly compatible ionic radius of F^- (1.36 Å) and O^{2-} (1.40 Å), resulting in seriously preventing lattice distortion and increase electron transport properties in ZnO NRs [17], [26]. Furthermore, since the most useful approach to minimize electron trap sites is to passivate defects and dangling bonds at the surface and grain boundaries, the F passivation effect as dopant in ZnO crystals give insight to investigate the prospective of ZnO NSs for optoelectronic parameters enhancement [8].

Three-dimensional (3D) ZnO nano-microstructures (NMSs) are favoured over 1D ZnO for carrier transportation and charge separation, because of their large surface area. Hence, the trisodium citrate (TSC) was chosen due to its ability in improving thin film adhesion to the substrate significantly and growth of various morphologies of different sizes (3D) with improved UV emission and decreased visible defect emission following TSC addition utilizing a simple approach, reducing

the complexity and expense of hybrid structure and nanocomposite synthesis, which is paramount for employment in a variety of applications [46]–[48].

This has prompted new research into the effects of fluorine doping on the fabrication and characterization of efficient ZnO-based MSM PDs. PDs based on fluorine-doped ZnO NRs with low power and rapid response are also uncommonly reported.

1.3 Aim and Objectives

This thesis aimed at the synthesis of undoped and F-doped ZnO nanorods (NRs) using modified hydrothermal-chemical bath technique for potential UV MSM PD. Also, the effect of trisodium citrate (TSC) additive on the properties of F-doped ZnO was studied to offer further research works on other potential applications. Finally, the effect of fluorine and silver co-doping in ZnO was investigated and UV MSM PD was fabricated based on F-doped and F and Ag co-doped ZnO.

The objectives of the thesis are as follows;

1. To synthesize undoped and F-doped ZnO NRs using the modified hydrothermal-chemical bath method.
2. To fabricate UV MSM photodetector based on undoped and F-doped ZnO.
3. To study the effect of trisodium citrate (TSC) additive on the properties of F-doped ZnO.
4. To compare the photoresponse characteristics of UV MSM PD based on F-doped ZnO and silver and F co-doped ZnO.

1.4 Originality of the Study

The originality of this research study can be summarized as follows;

1. Synthesis of F-doped ZnO NRs using the modified hydrothermal-chemical bath method.
2. Study the effect of annealing temperature of F-doped ZnO NSs in air.
3. Enhancement of UV MSM PD characteristics using fluorine doping by modified hydrothermal-chemical bath method.
4. Understanding of effect of TSC on F-doped ZnO characteristics.
5. Realization of UV-C absorption using silver and fluorine co-doping.
6. Investigation of silver, fluorine co-doping on ZnO properties.
7. Comparison study of MSM UV PDs based on F-doped ZnO PD and fluorine and silver co-doped ZnO PD.

1.5 Scope of the Study

In this study, undoped and F-doped ZnO NRs were grown using modified hydrothermal-chemical bath method with ammonium fluoride (NH_4F) as the F source on a silicon substrate. The effect of F-doping on the properties of ZnO NRs was investigated. The effect of annealing temperature on the optimum F-doped ZnO NRs was further studied and characterized. The UV MSM photodetector based on undoped and F-doped ZnO NRs were fabricated. The effect of TSC additive on the properties of F-doped ZnO was investigated. Also, the effect of silver, fluorine co-doping in ZnO NSs was studied and characterized. Finally, comparison of the fabricated FZO and FAZO PDs were made.

1.6 Thesis Outline

This thesis is divided into six chapters and is structured as follows: The **first chapter** presented a brief introduction of ZnO nanostructures including its importance, synthesis methods, applications and importance of fluorine as dopant in ZnO. Also, problem statement, research objectives, originality of the study, thesis scope were further described. **Chapter 2** gave literature overview on the general features of ZnO NSs, hydrothermal method employed in ZnO synthesis, effect of F-doping in ZnO properties and F-doped ZnO NSs growth using both physical and chemical methods. In addition, the MSM UV-PD and sensing mechanisms were reviewed. **Chapter 3** presented the methodology employed for the synthesis, techniques and apparatus utilized to examine the prepared material and the fabricated MSM UV-PDs. **Chapter 4** described the results discussion of the effect of F-doping concentrations in ZnO, effect of annealing temperature on the optimized F-doped ZnO. The UV MSM PD of undoped and F-doped ZnO NSs were fabricated and characterized. **Chapter 5** described the characterization results of the TSC additive on the properties of optimized F-doped ZnO. Also, the effect of silver, fluorine co-doping in ZnO NSs was studied and characterized. Nonetheless, comparison of the fabricated FZO and FAZO PDs were made. Finally, in **Chapter 6**, the summary of findings of this study along with recommendations for further research were provided.

CHAPTER 2

LITERATURE REVIEW AND THEORETICAL BACKGROUND

2.1 Introduction

ZnO has wide bandgap (3.37 eV in bulk at RT), 60 meV binding energy, inexpensive, and thermal stability made it widely investigated as gas sensor, UV PD and solar cell. This chapter summarized and reviewed articles related to the literature on the general features of ZnO material, hydrothermal method employed in ZnO synthesis, effect of F-doping in ZnO properties and F-doped ZnO NSs growth using both physical and chemical methods, and effect of trisodium citrate on the growth of ZnO material. In addition, the MSM UV-PD and sensing mechanisms were reviewed. Finally, the fundamental mathematical equations for photoresponse properties were also presented.

2.2 Crystal Structure of ZnO

Zinc oxide (ZnO) is a majorly inorganic compound that exists as white color powder, insoluble in water and it consists of zinc (Zn) and oxygen (O) which are readily available, most ample/ abundant beneath earth surface/crust at a large quantity of 4.61 x 10^5 ppm and 70 ppm for O and Zn, respectively [2]. It exists in three (3) different type of crystal structures namely; Wurtzite, Zinc blende, and Rock salt and these structures were presented in Figure 2.1. The wurtzite structure is the most stable structure thermodynamically at RT and ambient pressure. The crystalline wurtzite ZnO has a hexagonal unit cell with two lattice parameters ***a*** and ***c***, which fits /belongs to the space group of C_{6V}^4 /P6_3mc and there are 4 atoms per primitive cell which results to 12 degrees of freedom. The lattice parameters ***a*** and b of hexagonal

unit cells are the same and different with c, mostly ranging from 3.2475 to 3.2501 Å for ***a*** and from 5.2042 to 5.2075 Å for ***c*** [49], [50].

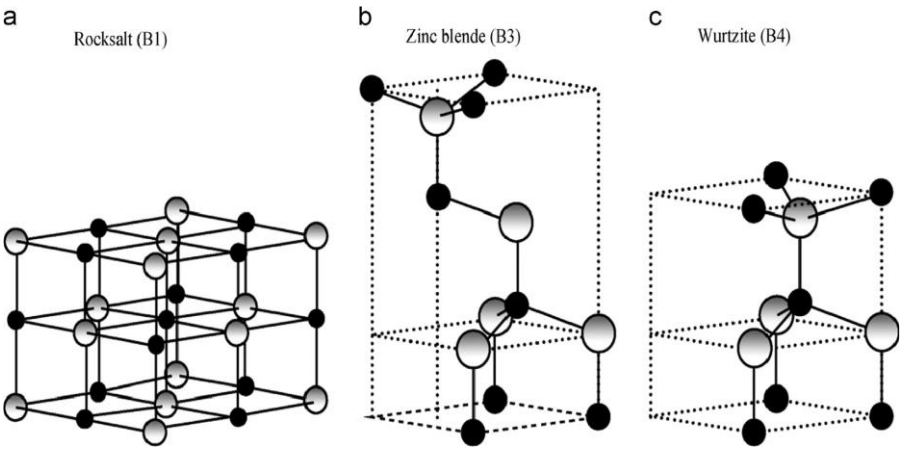

Figure 2.1: Stick-and-ball representation of ZnO crystal structures: (a) cubic rock salt (B1), (b) cubic zincblende (B3), and (c) hexagonal wurtzite (B4). Zn and O atoms, are denoted by the shaded gray and black spheres, respectively [15], [40].

ZnO NRs crystal structure is described by two interconnecting sublattices of O^{2-} and Z^{2+} ions which are tetrahedrally coordinated in a way that Zn ion surrounded by O ion and vice versa, stacked alternately along c-axis, where O^{2-} terminated O-$(000\bar{1})$ is the bottom surface and Zn^{2+} terminated (0001) is the top surface as shown in the Figure 2.2. There are two polar surfaces and two most common nonpolar surfaces associated with the ZnO crystal structure namely, polar O $(000\bar{1})$ and Zn (0001) terminated faces, and non-polar Zn (1120) and O (1010) terminated surfaces. The ZnO polar surfaces are a highly essential feature, because it possesses normal dipole moment in the c-axis caused as a result of the oppositely charged ions for Zn^{2-} and O^{2-}, resulting in positively charged (0001) and negatively charged $(000\bar{1})$ surfaces, respectively. Furthermore, the ± (0001) surfaces of ZnO are atomically stable, flat, and free of surface reconstruction, implying that the ZnO structure is fairly stable. Also, for ZnO the facets $\{2\bar{1}\bar{1}0\}$ and $\{01\bar{1}0\}$, are commonly non-polar

surfaces with lower energy than the facets {0001} [40], [49]. ZnO grown on the cubic substrate resulted in zinc blend stable structure phase and applied high pressure on wurtzite resulted to rock salt structure [50]. Piezoelectricity and pyroelectricity seen in ZnO are because of the non-centrosymmetric structure due to tetrahedral coordination [49]. The higher bandgap of the ZnO permits larger breakdown voltage and capacity for the sustainment of a huge electric field, the electronegativity of ZnO and Zn are 4.2eV and 0.99eV respectively [51], [52]. ZnO's low refractive index of 2.05 makes it easier for light to be extracted in many optical device applications. ZnO is a very solid and brighter excitonic-based ZnO emitter, owing to its far higher exciton binding energy of 60 meV, which is almost three times that of GaN (21 meV) (thermal energy at RT is around 25 meV). ZnO is a nontoxic semiconductor with a high redox potential, superior physical, chemical stability and has a strong radiation hardness with a threshold displacement energy of up to 30 eV (e.g., by far greater than 14 eV and 9 eV for Si and GaAs, respectively) [53], [54]. Table 2.1 shows the basic properties of ZnO.

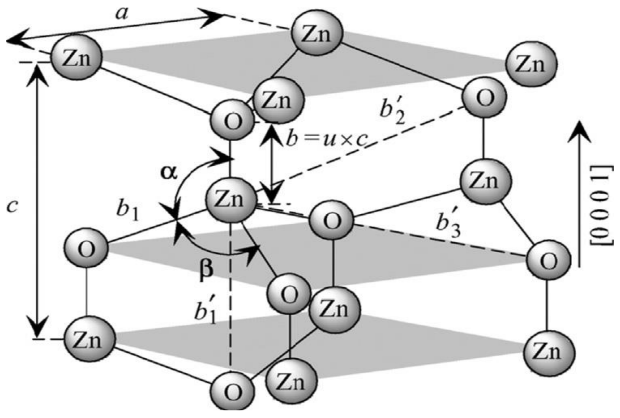

Figure 2.2: Schematic illustration of a wurtzitic ZnO structure with lattice constants **a** and **b**, in the basal plane and direction, respectively; u parameter is expressed as the bond length of the nearest-neighbor distance **b** divided by **c** 0.375 (for ideal crystal), α and β (109.47° in ideal crystal) are the bond angles and **b′₁, b′₂, b′₃** are three types of second-nearest-neighbor distances [15], [40].

Table 2.1: Basic Properties of ZnO [39], [50].

Parameters		Values
Crystal structures		Wurtzite, Rock Salt and Zinc-blende
Appearance		Amorphous white or yellowish-white powder
Nature of oxide		Amphoteric oxide
Stable at RT		Wurtzite
Lattice constants at 27^0C	a_0	0.32495 nm
	c_0	0.52098 nm
	c_0/ a_0	1.6033
Energy gap at RT		3.37 eV
Density		5.606 g/cm^3
Melting point		1975^0C
Solubility in water		0.16 mg 100 ml^{-1}
Exciton binding energy		60 meV
Refractive index		2.0041
Linear expansivity value (/^{0}C)		a_0: 6.5x10^{-6}
		c_0:3.0x10^{-6}
Static dielectric constant		8.656
Electron mobility at 300K		200cm^2 V^{-1} s^{-1}
Hole mobility at 300K		5-50cm^2 V^{-1} s^{-1}
Breakdown voltage (10^6Vcm^{-1})		5.0
Ionicity		62%
Electron effective mass		0.24m_0
Intrinsic carrier concentration		10^{16} to 10^{20} cm^{-3} maximum p-type doping 10^{17} cm^{-3}; maximum n-type doping 10^{20} cm^{-3}

2.3 Optical Properties of ZnO

ZnO is of considerable interest in semiconductor industry due its important and unique qualities of huge 3.37 eV direct wide bandgap, 60 meV large exciton bond energy at RT, and strong light absorption ability [12], [13]. Hence, ZnO is a very promising and advantageous materials for a wide range of applications in nano-

device technology, including UV detectors, bio-imaging, photocatalysis, cancer treatment, biosensors, detection of metal ions, and optoelectronics [55].

In general, higher luminescence is observed in direct band gap materials than indirect band gap materials, and big band gap materials are advantageous in lowering device leakage current. The two main reasons for bandgap narrowing or widening as a semiconductor is doped anionically or cationically are; (i) increase in carrier density which rises/raises the Fermi level close to conduction band due to Burstein-Moss shift [2], (ii) electron-impurity or electron-electron scattering as a result of doping leads to narrowing of band gaps due to the renormalization of bandgap [11].

Moreover, the photoluminescence (PL) analysis technique is a useful and promising in detecting, analysing optical characteristics, the crystal quality of semiconductor materials, defect states, and impurities in the emission band. PL may be employed to investigate structural defects generated by doping, including O vacancies or metal interstitials, which is majorly influential on oxide nanostructures' optical properties [4], [45]. The PL spectra of ZnO are divided into UV emission as near band emission (NBE) in UV range, which is associated with the ZnO characteristic emission and visible emission as deep-level emission (DLE) responsible for the existence of several defect states in the ZnO, such as ZnO (zinc antisite), Zn_v (zinc vacancy), Zn_i (zinc interstitial) O_{Zn} (oxygen antisite), O_v (oxygen vacancy) and O_i (oxygen interstitial) [48], [56], [57].

The ratio of the intensity of UV emission to the visible deep level emission (I_{UV}/I_{DLE}) is a vital metric for determining the crystal quality and quantity of defects in ZnO materials; the higher the intensity ratio, the better crystal quality. A large

difference in intensity indicates that the grown ZnO NRs arrays are of high quality, with few defects and a good hexagonal structure [5], [56].

2.4 Hydrothermal/Chemical Bath Method

Different synthesis methods have widely been developed and employed for the ZnO NSs growth such as metal-organic chemical vapor deposition [58], thermal evaporation [59], hydrothermal oxidation [57], print and fire method [60], electrochemical deposition [61], thermal chemical vapor deposition [62], and the hydrothermal method [10], [33], [34]. However, all of these techniques excluding hydrothermal method necessitate modern equipment and strict growing conditions. The hydrothermal/ chemical process is a simple, environmentally friendly (non-polluting) in large scalable, less expensive, more accessible, safer, and low-temperature method. Also, it yields films or powders of high crystal quality with a restricted size distribution and great purity without the need for high-temperature heat treatment [1], [4]–[6]. Furthermore, this technique makes it easier to control the size and morphology of the structures by changing the growth parameters (time, temperature, concentration, and dopants), and it can be used to fabricate optoelectronic devices on different types of substrates including flexible substrates. It can also be used to prepare technologically promising semiconductors with high device purity [12], [63], [64].

2.4.1 Disadvantages of Hydrothermal/Chemical Bath Method

Moreover, the wet chemical methods have some drawbacks which include: (i) the rate of growth in liquid-based processes is slower than the vapor-phase process. (ii) mandatory proper control of the concentration and pH of the electrolytes to

eliminate solvent incorporation into the electrolyte solution; (iii) mandatory use of seed layer deposition using a physical process such as spin coating or sputtering before actual synthesis, resulting in additional fabrication processes (iv) poor adhesion to the substrate due to low temperature [6], [48], [59].

2.4.2 Hydrothermal/Chemical Bath Method Growth Mechanism

When synthesizing ZnO thin films, it's crucial to keep track of the optimum orientation for each application. The (002) orientation of ZnO normal to the substrate is critical for piezoelectric applications, however the (100) orientation is useful for transparent conductive oxide (TCO) applications because of the larger grain size than (002) orientation films [11], [65]. For the growth of well-aligned NRs or nanowires on the substrate, a ZnO thin film seed layer in the range of 10-70nm is needed which serves as a guide, for nucleation mechanism and growth direction [66], [67]. As a seed layer, a textured ZnO nanocrystal or ZnO thin film is utilised, and techniques such as ALD, sol-gel, and sputtering processes are commonly used. The grain boundaries and the surface of the seed layer are commonly two important conditions where the nucleation process occur, the right choice of seed layer plays an important role in the alignment and length of the ZnO NRs because it significantly minimizes the lattice distortion/mismatch between the substrates and NRs which consequently yield well-aligned growth NRs on the substrates [68]. The growth parameters (pH, precursors concentration, seed layer, and growth temperature) are the key factors upon which aspect ratio depends (length/diameter). The Zn hydrate solubility and the dopant material hydrate are the determinant key factors for the doped ZnO 1D-NS morphology and dopant concentration.

The ZnO NRs synthesis is produced based on the following reaction equations in an aqueous solution of zinc salts like zinc nitrate ($Zn(NO_3)_2$) and organic amine such as hexamethylenetetramine (HMT=$C_6H_{12}N_4$). HMT is commonly called methenamine, which is a nonionic tetradentate cyclic tertiary amine usually used in the hydrothermal method due to its high solubility in water and it provides hydroxyl group, keeps neutrality behaviour of solution at pH7 for the formation of ZnO [67]. Hydroxyl ions are released by thermal degradation. These hydroxyl ions then react with Zn^{2+} ions and dopants to form doped ZnO. NaOH, KOH, NH_4OH, or Ammonia water is added into the solution for pH adjustment of the solution in ZnO growth to the desired value [12], [53]. The hydrothermal growth mechanism of ZnO nanostructures is described in Equations (2.1-2.7), [33], [69], [70]: Equation (2.1) represents dissolution of the $Zn(NO_3)_2.6H_2O$ salt into zinc ions.

$$Zn(NO_3)_2.6H_2O_{(s)} \rightarrow Zn^{2+}{}_{(aqs)} + 2NO^{3-}{}_{(aqs)} \quad (2.1)$$

HMT decomposes when heated to produce formaldehyde as seen in the chemical reaction, Equation (2.2).

$$C_6H_{12}N_{4_{(s)}} + 6H_2O_{(l)} \rightarrow 6CH_2O_{(aqs)} + 4NH_{3\ (aqs)} \quad (2.2)$$

Ammonia hydrolyses to yield ammonium ion and hydroxyl ion

$$NH_3 + H_2O \rightarrow NH_4{}^{+}{}_{(aqs)} + OH^{-}{}_{(aqs)} \quad (2.3)$$

Zinc hydroxyl is formed as the Zn^{2+} and OH^- ions concentration exceeds a certain critical value, then ZnO nuclei start to precipitate.

$$Zn^{2+}{}_{(aqs)} + 4OH^{-}{}_{(aqs)} \rightarrow Zn(OH)_4^{2-}{}_{(aqs)} \quad (2.4)$$

Dehydration of Zinc hydroxyl leads to the formation of ZnO crystals as in Equation (2.5).

$$Zn(OH)^{2-}_{4\,(aqs)} \rightarrow ZnO_{(s)} + H_2O_{(aqs)} + 2OH^-_{(aqs)} \quad (2.5)$$

The self-assembly of ZnO nuclei occurs to form rod-like NSs along preferred axis orientation under strong hydrothermal conditions, depending on growth circumstances.

Halo acid formation

$$NH_4F_{(s)} \rightarrow NH_3 + HF \quad (2.6)$$

the doping process is achieved by the chemical reaction between halo acid and grown ZnO shown below

$$ZnO + 2HF \rightarrow ZnF_2 + H_2O \quad (2.7)$$

2.5 ZnO NSs synthesized using Hydrothermal/Chemical Bath Method

The hydrothermal method uses water as the materials' solvent at elevated temperatures (100 to 200 ^{0}C) and pressure in closed vessels (mostly autoclaves) for the growth and crystallisation of nano-micro materials, whereas the CBD method is similar to the hydrothermal method except it takes place at ambient pressure (open vessels) and low temperature (less than 100 °C). Moreover, the synthesis mechanisms in both methods are the same [6], [71].

Anu Katiyar and his group [71] synthesized ZnO nanoflowers (NFLs) at low temperature of 95 ^{0}C for 4hrs using substrate free ultrasonic-assisted hydrothermal synthesis with the 0.1M equimolar solution of HMT and zinc nitrate hexahydrate in

DI water. They used a low-cost Borosil autoclave bottle instead of expensive teflon-lined stainless-steel autoclave for the growth process in a muffle furnace. They produced ZnO NFLs consisting petal like of various arranged hexagonal shaped NRs with the length of (100-150 nm) and diameter of (30-70 nm).

Shabannia and Abu Hassan studied the effect of various concentrations (0.025, 0.05, 0.075, and 0.1 M) on the 70 nm ZnO seeded polyethelene naphthalate (PET) substrate using CBD method. Equimolar concentration of zinc nitrate hexahydrate and HMT were dissolved separately in a beaker containing DI water to obtain precursor solution concentration. The CBD process was done by placing the prepared solution and substrate in the beaker to the preheated oven at 95 ^{0}C for 5 hrs. They found that the ZnO NRs' morphology, structural and optical properties were affected by the precursor concentrations. However, they found well-aligned hexagonal ZnO NRs with the average diameter in the range of 10 to 40 nm and sharpest, most intense UV peaks at 0.05 M precursor concentration [72].

Abuelsamen and his group [73] investigated various precursor concentrations impact on the optical and morphological properties of ZnO NRs on the 100 nm seeded glass substrate. The precursor solution is made of zinc nitrate hexahydrate and HMT and were dissolved separately in a beaker containing DI water to obtain precursor solution concentration. The synthesis process was done using CBD method in a preheated oven at 90 ^{0}C for 3hrs. They found that increasing the concentration had a significant impact on the crystal quality and surface morphology of ZnO NRs, as well as on UV photosensing. The ZnO NRs density dropped as the precursor concentrations grew. The greatest photocurrent and current gain under low power intensity for MSM UV PD were obtained at 0.05 M precursor concentration.

Sy-Hann Chen et al synthesized vertically arranged ZnO NR employing CBD method with the zinc acetate and HMT as a precursor solution in DI water on gallium-doped ZnO substrate deposited by pulse layer deposition. They investigated the influence of varying the concentrations in the range (0.01 to 0.07 M) and realized increment in intensity, average length and diameter with the increase of concentration. It was revealed that 0.05 M concentration have shown highest aspect ratio [74].

Abdulrahman and his group studied the influence of varying precursor concentration on the synthesis and characteristic properties of ZnO NRs grown using modified and conventional CBD techniques. The growth process was done using 100 nm ZnO seeded glass substrate with the zinc nitrate hexahydrate and HMT solution as precursor at different concentrations (0.01, 0.025, 0.05, and 0.075 M). They found that the characteristics properties of ZnO NRs synthesized employing the modified CBD method were remarkably enhanced with the precursor concentration increment. Also, they found that the synthesis of ZnO NRs employing modified CBD technique at 0.05 M have shown much higher aspect ratio of 25 as compared to the 11 for the one synthesized using conventional CBD method. Furthermore, the characteristic properties obtained in both methods at 0.05 M have favourably revealed the best results in terms of morphology, structural and optical properties [75].

Bidier et al [76] grew ZnO NRs on glass substrate using CBD method. The precursor solution was made up of 0.2 M equimolar concentration of zinc nitrate hexahydrate and HMT and dissolved in 80 mL DI water in a beaker. The CBD process was done in a furnace oven at 93 ^{0}C for 5 hrs. They investigated the influence of post annealing temperatures (PAT) (300, 400, and 500 ^{0}C) in ambient air

for 1hr. They observed that 400 ^{0}C as the optimum PAT for the enhancement of the morphological, structural and optical properties for better crystal quality.

Nonetheless, it revealed from literature survey that 0.05M concentration shows promising result in the crystal quality enhancement and device performance. Therefore, it can be employed in this thesis for doping process to harvest the established importance for better material properties and enhanced optoelectronics.

2.6 Doping Process in Semiconductor

The introduction of small quantities of impurities into a pure semiconductor, causes material's characteristics to alter from its native form and the process is termed as doping. The introduced impurities result to some defects that can alter the materials' morphology, structure, compositions, electrical and optical properties [22], [77].

The doping process is classified into two types namely: the p-type and n-type, which can be shown in Figure 2.3. In p-type doping, the dopant atoms have more valence electrons than that of the host material, as such the dopant atoms gain electrons from the host, creating acceptor levels above the valence band (VB). These acceptor impurity atoms accept electron from the VB. However, in case of n-type doping, the atom to be replaced has valence electron less than that of the dopant atom. Hence, additional extra free electron can be provided to the host material, creating excess negative electron as impurity. These set free electrons impurity created CB which will result in the electrical and optical properties enhancement [78].

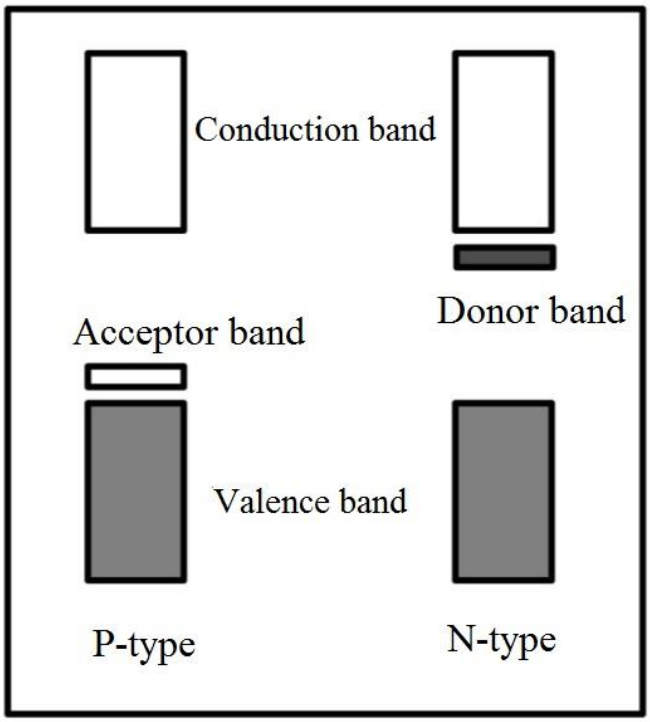

Figure 2.3: Illustrative diagram of the type of doping in ZnO [78].

2.7 F-doped ZnO

The growth of fluorine-doped ZnO is done by different precursors such as benzoyl fluoride (C_6H_5COF) [79], zinc fluoride (ZnF_2) [27] sodium fluoride (NaF) [16], [26] tetrafluoromethane (CF_4) [30], [80], ammonium hydrogen fluoride (NH_4FHF) [34], hydrofluoric acid (HF) [81] ammonium fluoride (NH_4F) [17], [28], [32], [82]. The NH_4F is the most widely used for fluorine-doped ZnO synthesis due to it is stability, safety in preparation than other dopant precursors.

2.7.1 Importance of Fluorine as Dopant

Fluorine doping in ZnO NSs film has many benefits over other dopants, including abundance, low cost, as well as the atomic radii size compatibility of the oxygen and fluorine atoms, resulting in minimal or negligible conduction band perturbation [83]. F^- can effectively facilitate precursor solubility; it increases

solution chemical potential, which favours nanostructure (NS) growth and reduces material resistance, resulting in improved conductivity. Also, it does improve the mobility of carrier ions by lowering the viscosity of the solution, resulting in increased conductivity, which prevents recombination by not trapping electrons [27]–[31].

2.7.2 Effect of F on Properties of ZnO

Doping of F into ZnO crystals could change the morphology, structure, optical, and electrical properties of the ZnO. This section presents the effects of F-doping on the properties of ZnO. The F atom, being the most electronegative element, substitutes O when it is doped into the ZnO matrix with the minimal lattice perturbation because of their comparable atomic radii [17], [26]. At lower concentrations, F occupies oxygen sites, causing decrement of the lattice parameter (*c*) because O has a greater radius than F, while at greater concentrations, it occupies interstitial sites, resulting in increment of *c* [84].

The F-doping mechanisms in ZnO can be summarized in Figure 2.4 and Equations (2.8) - (2.10) as follows:

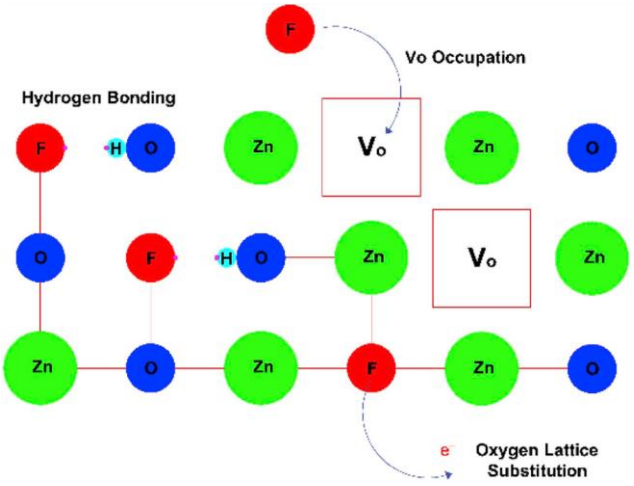

Figure 2.4: The schematic illustration of F inclusion on the ZnO matrix [8], [85].

$$Zn_{Zn}^{x} + O_{0}^{x} \leftrightarrow V_{Zn}^{x} + V_{0}^{x} + ZnO(s) \quad (2.8)$$

$$O_{0}^{x} + F_{0}^{x} \leftrightarrow {}^{1}/_{2}\, O_{2} + F_{0}^{\circ} + e^{x} \quad (2.9)$$

$$V_{0}^{-} + 2e^{/} + F_{0}^{x} \leftrightarrow F_{0}^{\circ} + e^{/} \quad (2.10)$$

Firstly, Equation (2.8) showed the settlement or occupation of F^- ion in the oxygen vacancies. Secondly, Equation (2.9) explained the substitution of O atom by F^- ion because of their comparable atomic radii (i.e F^- (1.36 Å), O^{2-} (1.40 Å)). Thirdly, Equation (2.10) explained the generation of hydrogen bonding with the OH groups by F atom due to its high electronegativity. Therefore, from the foregoing equations (2.8-2.10) it was concluded that F^- generates an electron in ZnO matrix, causing carrier concentration increment [8], [85].

The F-doping process affects the electrical properties of ZnO. Liu and his group employed first-principles for the investigation of F-doping in ZnO films and confirmed the carriers and mobility enhancement at the low F concentration doping due to the surface passivation impact of F [31]. Xu et al. have demonstrated that F-passivation of ZnO nanocrystalline through passivating defects and surface dangling bonds, resulted in increment of carrier concentration, mobility and very low resistivity for ZnO [27].

Cao and group demonstrated pulsed laser deposition of very transparent conducting F-doped ZnO (FZO) thin films on glass substrates. For the deposited F-doped ZnO films at an ideal oxygen pressure of 0.1 Pa, a small resistivity, carrier concentration and hall mobility of 4.83 $x10^{-4}$ Ω cm, 5.43 $x10^{20}$ cm^{-3} and 23.8 cm^2 V^{-1} s^{-1} were found. Over the whole visible wavelength range, the average optical